A New FDTD Algorithm Based on Alternating-Direction Implicit Method

Takefumi Namiki, *Member, IEEE*

***Abstract*— In this paper, a new finite-difference time-domain (FDTD) algorithm is proposed in order to eliminate the Courant–Friedrich–Levy (CFL) condition restraint. The new algorithm is based on an alternating-direction implicit method. It is shown that the new algorithm is quite stable both analytically and numerically even when the CFL condition is not satisfied. Therefore, if the minimum cell size in the computational domain is required to be much smaller than the wavelength, this new algorithm is more efficient than conventional FDTD schemes in terms of computer resources such as central-processing-unit time. Numerical formulations are presented and simulation results are compared to those using the conventional FDTD method.**

***Index Terms*—ADI method, CFL condition, FDTD method.**

I. Introduction

IT IS WELL known that the finite-difference time-domain (FDTD) method [1], [2] is a very useful numerical simulation technique for solving problems related to electromagnetism. However, as the traditional FDTD method is based on an explicit finite-difference algorithm, the Courant–Friedrich–Levy (CFL) condition [2] must be satisfied when this method is used. Therefore, a maximum time-step size is limited by minimum cell size in a computational domain, which means that if an object of analysis has fine scale dimensions compared with wavelength, a small time-step size creates a significant increase in calculation time.

In this paper, a new algorithm is proposed in order to eliminate the restraint of the CFL condition. This new algorithm is based on the alternating-direction implicit (ADI) method [3], [4] and is applied to the Yee's staggered cell to solve Maxwell's equation. The ADI method is known as the implicit-type finite-difference algorithm, which has the advantage of ensuring a more efficient formulation and calculation than other implicit methods in the case of multidimensional problems. We have called this new algorithm the ADI FDTD method. In Section II, numerical formulation of the ADI FDTD method for a two-dimensional (2-D) TE wave is presented. In Section III, the numerical stability of the formulation is derived. In Section IV, the numerical dispersion of the formulation is studied analytically. In Section V, numerical examples are presented and compared to those using the conventional FDTD method.

Manuscript received July 15, 1998.

The author is with the Computational Science and Engineering Center, Fujitsu Limited, Chiba 261-8588, Japan.

Publisher Item Identifier S 0018-9480(99)07709-1.

II. Numerical Formulation for a 2-D TE Wave

The numerical formulation of the ADI FDTD method for a 2-D TE wave is presented in (1)–(6). In order to simplify the problem, we have assumed that the medium in which the wave propagates is a vacuum. In addition, we have assumed that all cells in a computational domain have the same size. The electromagnetic-field components are arranged on the cells in the same way as that using the conventional FDTD method. The calculation for one discrete time step is performed using two procedures. The first procedure is based on (1)–(3) and the second procedures is based on (4)–(6).

First Procedure:

$$E_x^{n+1/2}(i+1/2,j) = E_x^n(i+1/2,j)+\left(\frac{\Delta t}{2\varepsilon\Delta y}\right)\cdot\left\{H_z^n(i+1/2,j+1/2\ -H_z^n(i+1/2,j-1/2)\right\} \quad (1)$$

$$E_y^{n+1/2}(i,j+1/2) = E_y^n(i,j+1/2)-\left(\frac{\Delta t}{2\varepsilon\Delta x}\right)\cdot\left\{H_z^{n+1/2}(i+1/2,j+1/2)-H_z^{n+1/2}(i-1/2,j+1/2)\right\} \quad (2)$$

$$H_z^{n+1/2}(i+1/2,j+1/2) = H_z^n(i+1/2,j+1/2)+\left(\frac{\Delta t}{2\mu\Delta y}\right)\cdot\left\{E_x^n(i+1/2,j+1)-E_x^n(i+1/2,j)\right\}-\left(\frac{\Delta t}{2\mu\Delta x}\right)\cdot\left\{E_y^{n+1/2}(i+1,j+1/2)-E_y^{n+1/2}(i,j+1/2)\right\}. \quad (3)$$

Second Procedure:

$$E_x^{n+1}(i+1/2,j) = E_x^{n+1/2}(i+1/2,j)+\left(\frac{\Delta t}{2\varepsilon\Delta y}\right)\cdot\left\{H_z^{n+1}(i+1/2,j+1/2)-H_z^{n+1}(i+1/2,j-1/2)\right\} \quad (4)$$

$$E_y^{n+1}(i,j+1/2) = E_y^{n+1/2}(i,j+1/2)-\left(\frac{\Delta t}{2\varepsilon\Delta x}\right)\cdot\left\{H_z^{n+1/2}(i+1/2,j+1/2)-H_z^{n+1/2}(i-1/2,j+1/2)\right\} \quad (5)$$

0018–9480/99$10.00 © 1999 IEEE

$$H_z^{n+1}(i+1/2,j+1/2) = H_z^{n+1/2}(i+1/2,j+1/2)+\left(\frac{\Delta t}{2\mu\Delta y}\right) \cdot\left\{E_x^{n+1}(i+1/2,j+1)-E_x^{n+1}(i+1/2,j)\right\} -\left(\frac{\Delta t}{2\mu\Delta x}\right)\left\{E_y^{n+1/2}(i+1,j+1/2)-E_y^{n+1/2}(i,j+1/2)\right\}. \tag{6}$$

In the first procedure, the E_y component on the left-hand side and the H_z components on the right-hand side, as shown in (2), are defined as synchronous variables. Also, the H_z component on the left-hand side and the E_y components on the right-hand side, as shown in (3), are also defined as synchronous variables. Equation (2) cannot be used for direct numerical calculation, so that (2′) leads from (2) and (3) by eliminating the $H_z^{n+1/2}$ components. In the suffix "i," (2′) indicates the i maximum number of simultaneous linear equations. There after, (3) can calculate directly using the $E_y^{n+1/2}$ components calculated by (2′) as follows:

$$E_y^{n+1/2}(i-1,j+1/2)-\left\{\left(\frac{2\sqrt{\varepsilon\mu}\Delta x}{\Delta t}\right)^2+2\right\} \cdot E_y^{n+1/2}(i,j+1/2)+E_y^{n+1/2}(i+1,j+1/2) =-\left(\frac{2\sqrt{\varepsilon\mu}\Delta x}{\Delta t}\right)^2 E_y^n(i,j+1/2)+\left(\frac{2\mu\Delta x}{\Delta t}\right) \cdot\left\{H_z^n(i+1/2,j+1/2)-H_z^n(i-1/2,j+1/2)\right\} +\left(\frac{\Delta x}{\Delta y}\right)\left\{E_x^n(i+1/2,j+1)-E_x^n(i+1/2,j) +E_x^n(i-1/2,j)-E_x^n(i-1/2,j+1)\right\} \tag{2′}$$

In the second procedure, the E_x component on the left-hand side and the H_z components on the right-hand side, as shown in (4), are defined as synchronous variables. Also, the H_z component on the left-hand side and the E_x components on the right-hand side, as shown in (6), are also defined as synchronous variables. Equation (4) also cannot be used for direct numerical calculation, so that (4′) leads from (4) and (6) by eliminating the H_z^{n+1} components. In the suffix "j," (4′) indicates j maximum number of simultaneous linear equations. There after, (6) can calculate directly using the E_x^{n+1} components calculated by (4′) as follows:

$$E_x^{n+1}(i+1/2,j-1)-\left\{\left(\frac{2\sqrt{\varepsilon\mu}\Delta y}{\Delta t}\right)^2+2\right\} \cdot E_x^{n+1}(i+1/2,j)+E_x^{n+1}(i+1/2,j+1) =-\left(\frac{2\sqrt{\varepsilon\mu}\Delta y}{\Delta t}\right)^2 E_x^{n+1/2}(i+1/2,j) +\left(\frac{2\mu\Delta y}{\Delta t}\right)\{H_z^{n+1/2}(i+1/2,j-1/2) -H_z^{n+1/2}(i+1/2,j+1/2)\}+\left(\frac{\Delta y}{\Delta x}\right) \cdot\left\{E_y^{n+1/2}(i+1,j+1/2)-E_y^{n+1/2}(i,j+1/2) +E_y^{n+1/2}(i+1,j-1/2)-E_y^{n+1/2}(i,j-1/2)\right\} \tag{4′}$$

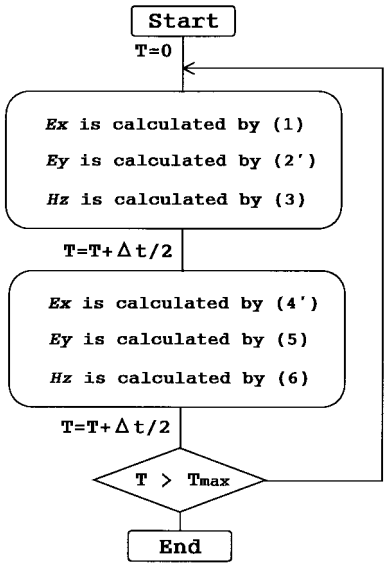

Fig. 1. Flowchart of the ADI FDTD method (2-D TE wave).

Since the simultaneous linear equations (2′) and (4′) can be written in tri-diagonal matrix form, the computational costs are not very significant.

The basic flowchart of this algorithm is shown in Fig. 1.

III. Analytical Investigation of Numerical Stability

The numerical stability of the ADI FDTD method is studied analytically. A 2-D TE wave is defined as follows:

$$\psi=\psi_0\xi^{n'}\exp\left\{j(k_xx+k_yy)\right\}$$

where $j=\sqrt{-1}$, k_x and k_y are wavenumbers, and ξ indicates growth factor

$$\xi^{n'}=\exp\left\{\gamma\left(\frac{\Delta t}{2}\right)n'\right\} \tag{7}$$

where γ is a complex constant.

The E_x, E_y, and H_z components can be written as follows:

$$E_x=\psi_A\xi_l^{n'}\exp\left\{j(k_xx+k_yy)\right\} \tag{8a}$$

$$E_y=\psi_B\xi_l^{n'}\exp\left\{j(k_xx+k_yy)\right\} \tag{8b}$$

$$H_z=\psi_C\xi_l^{n'}\exp\left\{j(k_xx+k_yy)\right\} \tag{8c}$$

where suffix l indicates the calculation procedure ($l=1$ indicates the first procedure and $l=2$ indicates the second procedure).

In order to calculate ξ_1 for the first procedure, substitute these equations into (1)–(3), we then obtain

$$\psi_A\xi_1=\psi_A+j(\Delta t/\varepsilon\Delta y)\sin(k_y\Delta y/2)\psi_C \tag{9a}$$

$$\psi_B\xi_1=\psi_B-j(\Delta t/\varepsilon\Delta x)\sin(k_x\Delta x/2)\psi_C\xi_1 \tag{9b}$$

$$\psi_C\xi_1=\psi_C+j(\Delta t/\mu\Delta y)\sin(k_y\Delta y/2)\psi_A-j(\Delta t/\mu\Delta x) \cdot\sin(k_x\Delta x/2)\psi_B\xi_1. \tag{9c}$$

By eliminating $\psi_A-\psi_C$ of (9), we get

$$p\xi_1^2-2\xi_1+q=0 \tag{10}$$

where

$$p = 1 + (\Delta t^2/\varepsilon\mu\Delta x^2)\sin^2(k_x\Delta x/2) \tag{11a}$$
$$q = 1 + (\Delta t^2/\varepsilon\mu\Delta y^2)\sin^2(k_y\Delta y/2). \tag{11b}$$

By solving (10), the growth factor of the first procedure ξ_1 is

$$\xi_1 = \frac{1 \pm j\sqrt{pq-1}}{p}. \tag{12}$$

In order to calculate ξ_2 for the second procedure, inserting (8a)–(8c) into (4)–(6), we obtain

$$\psi_A\xi_2 = \psi_A + j(\Delta t/\varepsilon\Delta y)\sin(k_y\Delta y/2)\psi_C\xi_2 \tag{13a}$$
$$\psi_B\xi_2 = \psi_B - j(\Delta t/\varepsilon\Delta x)\sin(k_x\Delta x/2)\psi_C \tag{13b}$$
$$\psi_C\xi_2 = \psi_C + j(\Delta t/\mu\Delta y)\sin(k_y\Delta y/2)\psi_A\xi_2 - j(\Delta t/\mu\Delta x)\sin(k_x\Delta x/2)\psi_B. \tag{13c}$$

By eliminating $\psi_A - \psi_C$ of (13), we obtain

$$q\xi_2^2 - 2\xi_2 + p = 0. \tag{14}$$

By solving (14), the growth factor of the second procedure ξ_2 is

$$\xi_2 = \frac{1 \pm j\sqrt{pq-1}}{q}. \tag{15}$$

Finally, (12) and (15) yields ξ, which indicates the growth factor of the total procedure as follows:

$$|\xi| = |\xi_1\xi_2| = |\xi_1|\,|\xi_2| = \sqrt{\frac{q}{p}}\sqrt{\frac{p}{q}} = 1. \tag{16}$$

Equation (16) is always satisfied so that the ADI FDTD algorithm is stable in any case.

IV. Analytical Investigation of Numerical Dispersion

We now let $\gamma = j\omega$ of (7) and assume $\xi_1 = \xi_2 = \xi_l$ of (10) and (14). By adding (10) and (14), we then get

$$(p+q)\xi_l^2 - 4\xi_l + (p+q) = 0. \tag{17}$$

Equation (17) can be written as follows:

$$(p+q)\left(\xi_l + \xi_l^{-1}\right) - 4 = 0. \tag{18}$$

Making use of (7) and (11), we get

$$\xi_l + \xi_l^{-1} = \left(\xi_l^{1/2} - \xi_l^{-(1/2)}\right)^2 + 2 = -4\sin^2(\omega\Delta t/4) + 2$$
$$p + q = 2 + \left(\Delta t^2/\varepsilon\mu\Delta x^2\right)\sin^2(k_x\Delta x/2) + \left(\Delta t^2/\varepsilon\mu\Delta y^2\right)\sin^2(k_y\Delta y/2).$$

Putting them into (18), we obtain

$$\left[(1/\Delta x)\sin(k_x\Delta x/2)\right]^2 + \left[(1/\Delta y)\sin(k_y\Delta y/2)\right]^2 = \left[(1/c\Delta t')\sin(\omega\Delta t'/2)\right]^2\cos(\omega\Delta t') \tag{19}$$

where c is the speed of light and $\Delta t' = \Delta t/2$.

The dispersion relation for a 2-D plane wave in a vacuum is

$$k_x^2 + k_y^2 = (\omega/c)^2. \tag{20}$$

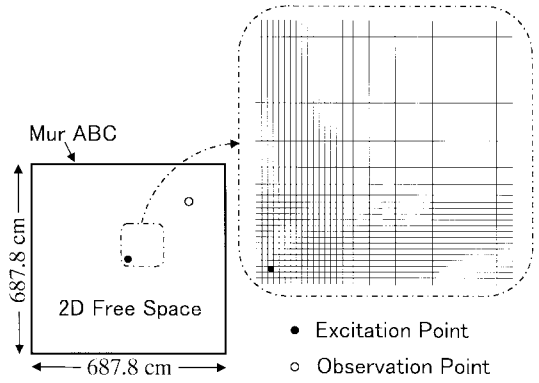

Fig. 2. 2-D free-space model.

It is revealed that the dispersion relations of (19) and (20) are identical in that the limit as Δx, Δy, and Δt all go to zero. This suggests that numerical dispersion of the ADI FDTD method can be reduced to any degree if appropriate cells are used.

V. Numerical Results

In order to demonstrate the above ADI FDTD method, a few numerical examples are presented. In the previous sections, we assumed a medium in which the wave propagated as a vacuum and the FDTD cell size was uniform. On the other hand, the ADI FDTD code for these demonstrations is made so as to treat inhomogeneous lossy medium and nonuniform cells. This technique is the same as that used in the conventional FDTD method. Numerical simulations are carried out using both the ADI FDTD method and the conventional FDTD method for comparisons.

A. 2-D Free-Space Model

A 2-D free-space model is shown in Fig. 2. The computational domain is 687.8 × 687.8 cm^2 (101 × 101 cells) and Mur's first-order absorbing boundary condition [5] are set on the outer surface. The cell size is set as follows:

$$\Delta(k)_{(\mathrm{mm})} = \begin{cases} 100.0 & (k = 1\text{–}32) & \Delta(k)\text{: constant} \\ 68.4 - 6.0 & (k = 33 - 39) & \Delta(k) = 1.5\Delta(k+1) \\ 4.0 & (k = 40 - 62) & \Delta(k)\text{: constant} \\ 6.0 - 68.4 & (k = 63 - 69) & 1.5\Delta(k) = \Delta(k+1) \\ 100.0 & (k = 70\text{–}101) & \Delta(k)\text{: constant} \end{cases}$$

where $\Delta(k) = \Delta x(i)$ for the x-direction and $\Delta(k) = \Delta y(j)$ for the y-direction. The excitation is applied at the H_z component of the central cell of the computational domain $(i = j = 56)$, and the excited waveform is as follows:

$$H_z = H_z + \sin^2\left(\frac{\pi t}{T}\right), \qquad T = 9.4\ \mathrm{ns} \tag{21}$$

The time-step size is set as 235.0 ps for the ADI FDTD method and 9.4 ps for the conventional FDTD method. The latter is decided as follows by the limitation of the 2-D CFL condition:

$$\Delta t \le \frac{1}{c\sqrt{(1/x)^2 + (1/y)^2}} \tag{22}$$

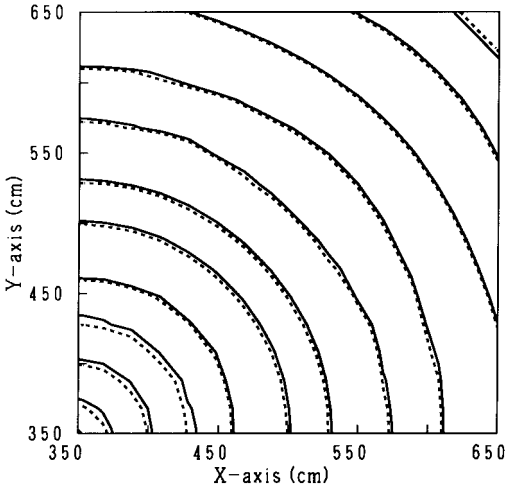

Fig. 3. Normalized H_z field distribution (solid lines: conventional FDTD, dotted lines: ADI FDTD).

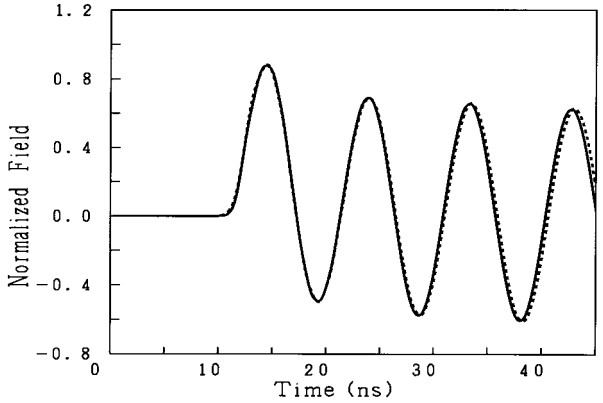

Fig. 4. Normalized H_z field in time domain (solid line: conventional FDTD, dotted line: ADI FDTD).

where x, y indicates minimum cell size (They are both 4.0 mm in this model). The total simulation time is set as 47 ns.

The H_z-field distribution in the upper right area of the computational domain is described by the contour lines of Fig. 3. The time is 21.15 ns after the start of excitation. The results of the ADI FDTD method and those of the conventional FDTD method are in good agreement.

The H_z-field normalized by a maximum value at observation point $(i = j = 90)$ is shown in Fig. 4. These results also agree very well.

These simulations are performed on a Ultra SPARC II 300-MHz workstation. The central-processing-unit (CPU) time and required memory of this simulation are shown in Table I with the time-step size and total time steps. In the case of the ADI FDTD method, the time-step size can be set 25 times as large as the conventional FDTD method and the total time steps can be reduced to 1/25. The CPU time is also reduced to 1/7.8. Required memory, which is about 1.3 times, is increased slightly because of the necessity of extra electromagnetic-field array storage.

B. Parallel-Plate Waveguide Model

The parallel-plate waveguide model that includes thin lossy dielectric films is shown in Fig. 5. The perfect electric conductor (PEC) boundary condition is applied on the surface of both plates. Mur's first-order absorbing boundary condition is applied at the terminal of the waveguide. There are 75×20 nonuniform cells in the computational domain, and the size of most cells is set as 1.0×1.0 mm^2. There are two films with 0.3-mm-wide slits in the waveguide. The films are 0.5-mm thick with electric characteristics of $\varepsilon_r = 2.0$, $\mu_r = 2.0$, and $\sigma = 15.0$ S/m. The minimum cell size is set as 0.1×0.1 mm^2 in order to treat the thin films and slits.

When we use the conventional FDTD method, the time-step size is set as 0.23 ps for this model because of the CFL condition requirement of the 2-D case shown in (22). When we use the ADI FDTD method, the time-step size is set as 3.33 ps.

The electric fields of vertical components in front of the left terminal are excited and that of the right terminal are observed

TABLE I

	Δt	Steps	CPU Time	Memory
Conventional	9.4 ps	5000	215.5 s	429.8 Kb
A D I	235.0 ps	200	27.5 s	566.7 Kb

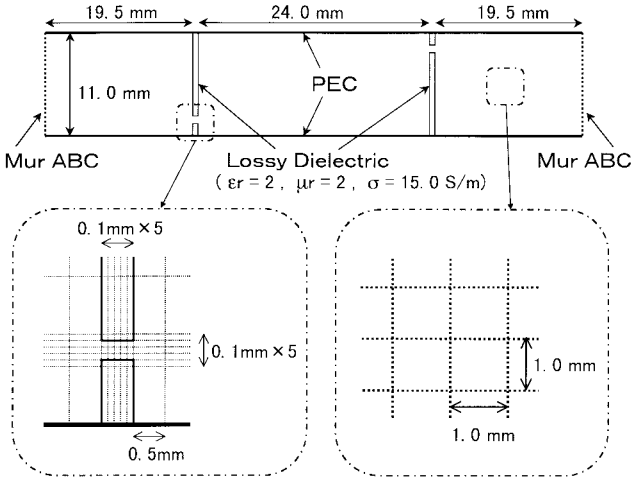

Fig. 5. Parallel-plate waveguide model.

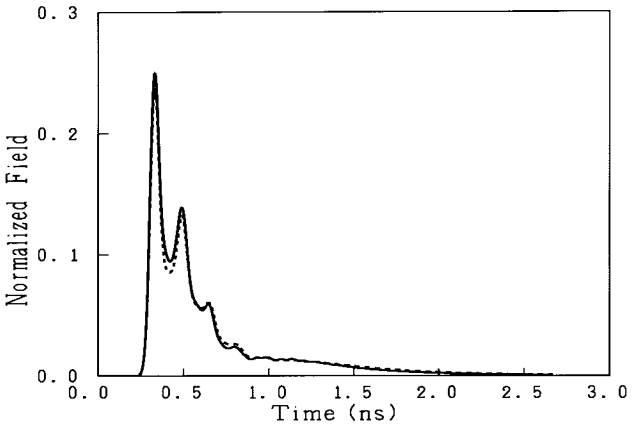

Fig. 6. Normalized output signal (solid line: conventional FDTD, dotted line: ADI FDTD).

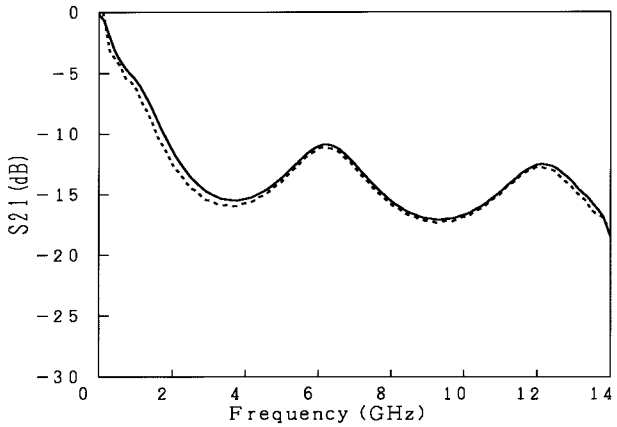

Fig. 7. Insertion loss (solid line: conventional FDTD, dotted line: ADI FDTD).

TABLE II

	Δt	Steps	CPU Time	Memory
Conventional	0. 23 ps	11600	63. 7 s	83.8 Kb
A D I	3. 33 ps	800	15. 1 s	104.8 Kb

as the output signal. The waveform of the excitation pulse is as follows:

$$E_y = E_y + \exp\left\{-\frac{(t-t_0)^2}{T^2}\right\}, \qquad t_0 = 120\ \text{ps}, T = 33\ \text{ps}.$$

The output signal normalized by the amplitude of the excited pulse is shown in Fig. 6. The results in the ADI FDTD and conventional FDTD are in quite good agreement. By applying the Fourier transformation of the excited pulse and output signal, the insertion losses are calculated. The results are shown in Fig. 7, and they also agree very well. Table II provides information on this simulation performed on the workstation. In the case of the ADI FDTD method, since the time-step size can be set 14.5 times as large as that of the conventional FDTD method, a total time step 1/14.5 of the conventional FDTD is sufficient. The CPU time of the ADI FDTD can then be reduced to 1/4.2 that of the conventional FDTD.

VI. Conclusion

This paper introduces a new FDTD scheme based on the ADI method. As this method is free from CFL condition restraint, it requires fewer computer resources, such as CPU time, if the minimum cell size in the computational domain is much smaller than the wavelength. Numerical simulation shows that the new method is very efficient, and the results agree very well with that of the conventional FDTD method.

In this paper, we have explained the ADI FDTD method for a 2-D TE wave. However, our explanation can also be applied to a 2-D TM wave and could be extended in a general sense to a full three-dimensional wave.

References

[1] K. S. Yee, "Numerical solution of initial boundary value problems involving Maxwell's equations in isotropic media," *IEEE Trans. Antennas Propagat.*, vol. AP-14, pp. 302–307, May 1966.
[2] A. Taflove, *Computational Electrodynamics*. Norwood, MA: Artech House, 1995.
[3] G. D. Smith, *Numerical Solution of Partial Differential Equations*. Oxford, U.K.: Oxford Univ. Press, 1965.
[4] D. W. Peaceman and H. H. Rachford, "The numerical solution of parabolic and elliptic differential equations," *J. Soc. Ind. Applicat. Math.*, vol. 3, pp. 28–41, 1995.
[5] G. Mur, "Absorbing boundary conditions for the finite-difference approximation of the time-domain electromagnetic field equations," *IEEE Trans. Electromag. Compat.*, vol. EMC-23, pp. 377–382, Nov. 1981.

Takefumi Namiki (M'99) was born in Chiba, Japan, on January 24, 1963. He received the B.E. degree in physics from Tohoku University, Sendai, Japan, in 1985, and is currently working toward the Ph.D. degree at Chiba University, Chiba, Japan.

From 1986 to 1991, he was with Fujitsu Laboratories Ltd., Atsugi, Japan, where he was engaged in research of high-speed optical modulator for optical communications systems. In 1991, he joined Fujitsu Ltd., Tokyo, Japan, where he was engaged in research and development of the computational science. Since 1994, he has been engaged in research of the computational electromagnetics. His research interests include numerical techniques for modeling electromagnetic fields and waves, and computer-aided engineering (CAE) system of microwave circuits, antennas, and optical waveguides.

Mr. Namiki is a member of the IEEE Antennas and Propagation (AP-S) and Microwave Theory and Techniques (MTT-S) Societies, and the Institute of Electronics, Information and Communication Engineers (IEICE), Japan.